ISBN: 978-3-95450-201-1 doi:10.18429/JACoW-IBIC2018-TUOC04

DEVELOPMENT OF BEAM POSITION MONITOR FOR THE SPring-8 UPGRADE

H. Maesaka†, RIKEN SPring-8 Center, 679-5148 Sayo, Hyogo, Japan
H. Dewa, T. Fujita, M. Masaki, S. Takano[1], Japan Synchrotron Radiation Research Institute, 679-5198 Sayo, Hyogo, Japan
[1]also at RIKEN SPring-8 Center, 679-5148 Sayo, Hyogo, Japan

Abstract

A precise and stable beam position monitor (BPM) system has been developed for the low-emittance upgrade of SPring-8. The requirements for the BPM system are: (1) a single-pass resolution of 100 μm rms for a 100 pC single-bunch and an electric center accuracy of 100 μm rms for the initial beam commissioning to achieve the first turn, (2) a closed-orbit distortion (COD) resolution better than 0.1 μm rms for a 100 mA stored beam and a position stability of less than 5 μm to maintain a photon beam axis. We designed a button electrode and a BPM block and produced some prototypes for performance evaluation. The development of readout electronics based on the MicroTCA.4 standard and the evaluation of a commercial electronics have also been conducted. The prototype BPM system was installed to the present SPring-8 storage ring to confirm the performance with an actual electron beam. We obtained sufficient signal intensity, electric center accuracy, position resolution, position stability, etc. by the beam test. Thus, the new BPM system is almost ready for the SPring-8 upgrade.

INTRODUCTION

SPring-8 has a low-emittance upgrade plan of the storage ring, SPring-8-II, to provide much more brilliant X-rays to users [1]. The beam energy is lowered to 6 GeV from the current 8 GeV and the lattice is changed to 5-bend achromat (5BA). As a result, the emittance is ~140 pm rad without radiation damping of insertion devices (IDs) and further reduced to ~100 pm rad by radiation damping of IDs, while the emittance of the present storage ring is 2.4 nm rad. The X-ray brilliance below 60 keV is expected to be more than 20 times higher than the present SPring-8 ring. In order to utilize brilliant X-rays, it is quite important to maintain the optical axis well within its intrinsic divergence by stabilizing the electron beam orbit. In addition, the beam orbit must be aligned to the magnetic center of each quadrupole or sextupole magnet at the commissioning stage to achieve the first beam storage, since the dynamic aperture of the new ring is narrower than the amplitude of closed orbit distortion caused by alignment error of magnets. Therefore, the resolution and the accuracy of the single-pass BPM measurement is crucial.

For the stability of the optical axis, the tolerances of the source point and the direction of X-rays are approximately 1 μm and 1 μrad, respectively, since the electron beam size is 28 (H) x 6 (V) μm^2 std. and since the divergence of X-rays is 5 (H) x 17 (V) μrad^2 std. for 10 keV photon energy. Thus, we set the closed-orbit distortion (COD) mode BPM stability to 5 μm peak-to-peak for 1 month. In this case, the angular stability of 1 μrad can be expected, because the distance between the two BPMs at the both ends of a straight section for an insertion device is 5 m.

For beam commissioning, the beam must be steered within a narrow dynamic aperture of approximately 10 (H) x 2 (V) mm^2. The required single-pass (SP) position resolution is 100 μm std. for a 100 pC single-bunch. Furthermore, the electric center of each BPM must be aligned within 100 μm std. (±200 μm max.) with respect to the magnetic center of an adjacent quadrupole magnet.

In order to satisfy these requirements, we designed a button BPM electrode, BPM block and readout electronics. Some prototypes of BPM components were produced and some of them have been tested with an actual electron beam at the present SPring-8 storage ring. In this article, we describe design of the BPM system, evaluation of prototypes, result of beam test, etc.

DESIGN AND BASIC PERFORMANCE OF THE BPM SYSTEM

BPM Electrode and Block

We took the following things into account for the design of a BPM electrode and block.

- Sufficient signal intensity for the SP-mode.
- Small heat generation by trapped modes etc.
- Nonmagnetic materials not to distort the field of adjacent magnets.
- Same cross-section as the vacuum chamber to be connected.

As a result, we designed a BPM electrode and block, as illustrated in Fig. 1.

Button electrodes are arranged on 20 mm-wide flat surfaces on the top and bottom of the vacuum chamber with a vertical aperture of 16 mm. The button diameter was set to 7 mm and the horizontal span of the electrodes was to 12 mm in order to obtain a signal as large as possible and to fit the electrodes to the flat top. Each electrode is inserted into the hole with 8 mm diameter, and hence the gap between the hole and the electrode is 0.5 mm. A cooling water channel is equipped with the block so as to suppress the temperature rise due to an electron beam.

We selected molybdenum for the material of the electrode. Since molybdenum has a good electric and thermal conductivity, the heat generation due to trapped modes can be reduced and the temperature rise can be sup-

† maesaka@spring8.or.jp

Content from this work may be used under the terms of the CC BY 3.0 licence (© 2018). Any distribution of this work must maintain attribution to the author(s), title of the work, publisher, and DOI.

ISBN: 978-3-95450-201-1 doi:10.18429/JACoW-IBIC2018-TUOC04

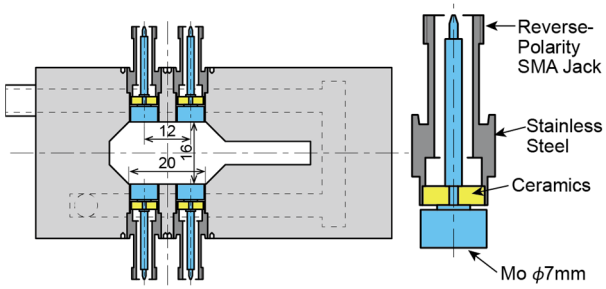

Figure 1: Schematic drawings of the BPM block (left) and the BPM electrode (right).

pressed. Since the thermal expansion coefficient of molybdenum is close to that of the insulator ceramics, it is easy to bond them together by brazing.

The material of the BPM block is stainless steel, which is the same as the other parts of the vacuum chambers. Since stainless steel has lower electrical conductivity than molybdenum, the stainless-steel part dissipates larger heat due to trapped modes than the molybdenum part. Each electrode is bonded to a block by electron-beam welding (EBW). This is because the heat input of EBW can be well controlled compared to TIG welding. Therefore, the shrinkage at the welded part is expected to be kept almost constant and the error on the electric center due to the button position difference can be suppressed.

The position sensitivity, the signal strength, trapped modes, etc. of the BPM were analyzed by using three-dimensional electromagnetic simulation code, CST Studio [2]. The position sensitivity coefficients, k_x and k_y, were computed to be 6.8 mm and 7.7 mm, respectively, when the beam position is calculated by,

$$\begin{pmatrix} X \\ Y \end{pmatrix} = \begin{pmatrix} \frac{k_x}{2}\left(\frac{V_1 - V_2}{V_1 + V_2} + \frac{V_4 - V_3}{V_4 + V_3}\right) \\ \frac{k_y}{2}\left(\frac{V_1 - V_4}{V_1 + V_4} + \frac{V_2 - V_3}{V_2 + V_3}\right) \end{pmatrix}.$$

Here, $V_1, \ldots, V_4$ are the signal intensities from the electrodes. The signal intensity from a 100 pC single-bunch was estimated to be –53 dBm at the acceleration frequency of 508.76 MHz with the bandwidth of 10 MHz. In this case, the SP-mode position resolution was expected to be 70 μm std., which is sufficient for the requirement. The signal intensity from a stored beam of 100 mA was estimated to be –12.5 dBm at 508.76 MHz, which was sufficient for the COD-mode position resolution of 0.1 μm std. at 1 kHz bandwidth.

The dimensions of the electrode were optimized so that the heat generation due to trapped modes was minimized. The detailed optimization process can be found in Ref. [3]. The heat dissipation in the optimized BPM electrode and block was calculated and plotted in Fig. 2. Although the natural bunch length after the upgrade is 7 ps rms, it will be longer than 10 ps for a 0.5 mA bunch current and longer than 14 ps for a 1 mA bunch current. Therefore, the heat generation in the BPM block was estimated to be 5 W maximum. The temperature of each part of the BPM block was analyzed by using ANSYS [4].

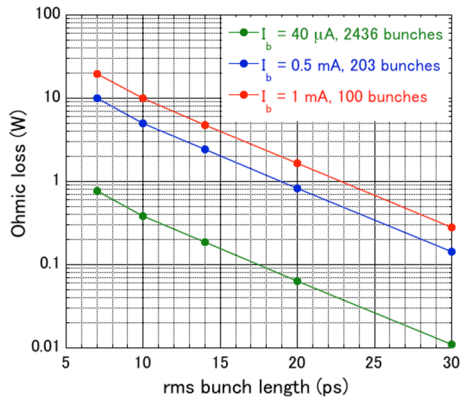

Figure 2: Calculated heat dissipation in the BPM block for the beam current of 100 mA with bunch currents of 0.04 mA (green), 0.5 mA (blue) and 1 mA (red) as functions of the bunch length.

When the BPM block is cooled by 30 ℃ cooling water, the maximum temperature of the electrode was estimated to be 35 ℃. Thermal deformation is expected to be sufficiently small for this temperature rise.

Prototype of BPM Electrode and Block

We ordered prototype BPM electrodes to two companies. The mechanical structure of the products from both companies are almost identical except for the slight difference in the shape of the ceramics part. The prototype electrodes were appropriately manufactured without any troubles, such as a vacuum leak. The machining error of both products was 10 μm level, which was small enough to fulfill the requirement for the electric center error. The mechanical strength and thermal cycle reliability were also confirmed to be sufficient. We measured Time-Domain Reflectometry (TDR) waveforms to check the RF characteristics. The data from both prototypes were almost identical and consistent with the simulation.

Some prototypes of BPM blocks were also produced. The machining accuracy was sufficient to satisfy the requirement for the electric center displacement (100 μm std., 2σ max.). The condition of the EBW process to attach electrodes to a block was investigated and optimized by using dummy electrodes and blocks. As a result, the shrinkage of the welded part was controlled within 50 μm and the corresponding electric center error was estimated to be less than 80 μm.

Signal Cable

The BPM system uses three types of signal cables serially connected, a short cable from the BPM block (A-cable), a long cable from the accelerator tunnel to the maintenance gallery (B-cable), and a short cable to the readout electronics (C-cable). The variation of the characteristics of these cables may cause a drift of the beam position. Therefore, the cables are necessary to be stable against irradiation, temperature change, etc.

From the operation experience of the SPring-8 BPM system, the stability of the A-cable is crucial for the BPM stability. In fact, some humidity-dependent drifts were

Content from this work may be used under the terms of the CC BY 3.0 licence (© 2018). Any distribution of this work must maintain attribution to the author(s), title of the work, publisher, and DOI.

ISBN: 978-3-95450-201-1 doi:10.18429/JACoW-IBIC2018-TUOC04

Content from this work may be used under the terms of the CC BY 3.0 licence (© 2018). Any distribution of this work must maintain attribution to the author(s), title of the work, publisher, and DOI.

found in the data from the present SPring-8 BPM system [5]. We found that the radiation damage to an A-cable caused the insulator to become moisture-absorptive. The characteristic impedance of the radiation-damaged A-cable was confirmed to be dependent on the humidity. Therefore, we selected SiO_2 and PEEK semi-rigid cables as radiation-resistant candidates for an A-cable. For the B-cable, a corrugated coaxial cable used in SPring-8 is a candidate.

To confirm the radiation hardness of the A-cable candidates, we placed samples of the A-cable in the tunnel of the current SPring-8 ring close to an X-ray absorber that scatters strong X-rays. As a result of irradiating the dose equivalent to the operation period of more than 10 years, we did not find any significant variation of characteristic impedance. Therefore, the candidates for the A-cable has sufficient resistance to radiation.

Readout Electronics

We select two candidates for the readout electronics: our original design based on MicroTCA.4 [6] and the new generation of Libera Brilliance+ [7]. They are developed and evaluated in parallel.

The hardware platform, MicroTCA.4, for the original electronics is same as the new low-level RF system for SPring-8 [8]. A schematic drawing is shown in Fig. 3. BPM signals are received by a BPM rear transition module (RTM), which is an RF frontend circuit having band-pass filters, amplifiers, step attenuators, baluns etc. The signals are transferred to a 10-channel digitizer advanced mezzanine card (AMC). The RF signal with the frequency of 508.76 MHz is directly sampled by a high-speed 16-bit ADC at 363 MSPS (under-sampling scheme). Since the number of active components for this scheme is small compared to other schemes, such as down-conversion, drifts of circuit components are expected to be small. In addition, BPM-RTM has calibration tone generators, each of which provides a calibration signal with a frequency slightly shifted from the beam signal.

As for Libera Brilliance+, we are evaluating the current product and discussing with the manufacturer about the specification of the new version. Required functions for the new version are a higher-order polynomial for beam position calculation, position calculation from three electrodes in case of a failure of signal from one of the four buttons, etc.

BEAM TEST

Setup

The prototype BPM system was installed to the present SPring-8 storage ring to confirm the performance with an actual electron beam. A schematic drawing of the BPM block for the beam test is shown in Fig. 4. The vertical aperture of the vacuum chamber is the same as that of upgraded ring, but the horizontal opening is fitted to the aperture of the present ring. The position of each BPM electrode is the same as the design for SPring-8-II. The BPM block is equipped with four BPMs separated by

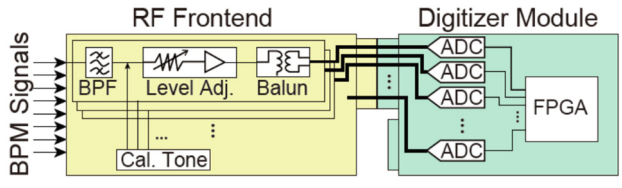

Figure 3: Schematic diagram of the MicroTCA.4-based BPM electronics.

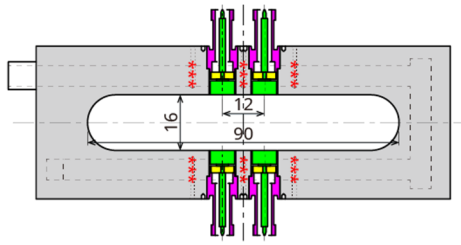

Figure 4: Schematic drawing of the BPM block for a beam test.

20 mm along the beam orbit, consisting of sixteen electrodes in total. A cooling water channel is embedded to maintain the temperature of the block. Some thermometers are inserted to holes around the electrodes (red *** part in the figure). The readout electronics is the current version of Libera Brilliance+.

Waveform and Intensity of Raw Signals

A signal waveform from a single bunch beam is shown in Fig. 5. A Bipolar impulse signal was appropriately obtained. Although some ringing can be seen, it disappears after 2 ns where the next bunch arrives. The signal intensity for a 100 mA stored current was –12.5 dBm at 508.76 MHz, which was consistent with the design value.

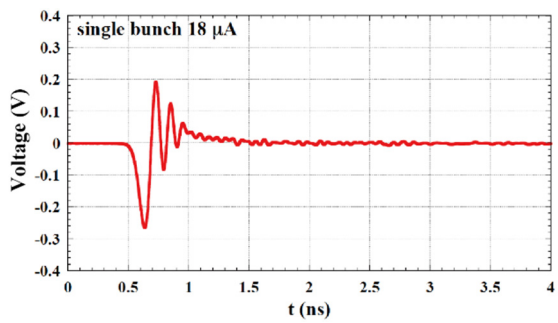

Figure 5: BPM signal waveform from a single-bunch electron beam.

Position Resolution

The position resolution was evaluated by comparing the data of the inside two BPMs with the line connecting the data from the outside two BPMs. The deviation of position data of one of the inside BPM to the reference value defined by the outside two BPMs is plotted in Fig. 6. The SP-mode data was taken with a 100 pC single- bunch and the position resolution was approximately 70 μm rms. The COD-mode data was taken with a 100 mA stored beam and the position resolution was about 0.01 μm rms. The position resolution is sufficient for our requirement of each detection mode.

ISBN: 978-3-95450-201-1 doi:10.18429/JACoW-IBIC2018-TUOC04

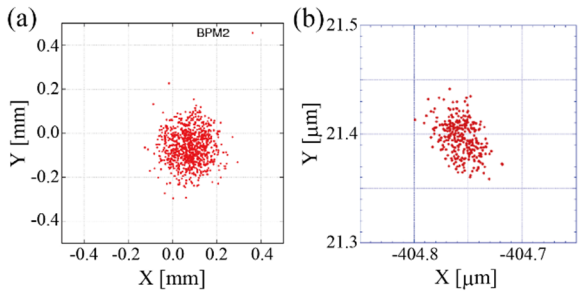

Figure 6: Beam position difference between a middle BPM data and the prediction from two BPMs at both ends. (a) is SP-mode data and (b) is COD-mode data.

Electric Center

The electric center precision was estimated by comparing the data from the four BPMs, as shown in Fig. 7. The beam position data from all the four BPMs are well within a circle of 0.1 mm radius. This result indicates that the electric center error is within 0.1 mm for the entire BPM system. Although the statistics is not enough, we expect that the electric center can satisfy 100 μm std. (2σ max.).

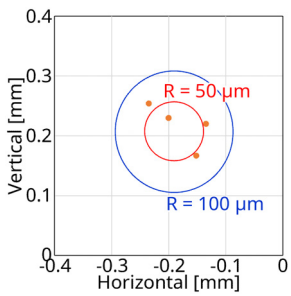

Figure 7: Beam positions from 4 BPM sets.

Long-term Stability

We use beam position values calculated from three electrodes to evaluate the long-term stability. There are four combinations to select three electrodes and the position value from each combination is ideally identical. We define balance error as the maximum difference among the four values [5]. If the balance error shows drifts, we suspect some drifts of the BPM system.

A trend graph of the balance error is plotted in Fig. 8. Since the filling pattern was changed every 2 weeks or so, the balance error showed small jump at that time. For a constant beam condition, the fluctuation of the balance error was within 5 μm. Thus, the long-term stability satisfies the requirement of 5 μm peak-to-peak.

Temperature Rise

The temperature around the BPM electrode was recorded during the beam test. The temperature difference with and without a beam was 0.1–0.5 °C, depending on the thermometer position and filling pattern. This result was consistent with the thermal analysis result by using ANSYS within 0.15 °C. Therefore, the heat input estimation and the thermal analysis are considered to be performed with sufficient accuracy. According to the thermal simulation, the hottest part is the molybdenum button electrode and its temperature is 35 °C. Since the temperature rise of the BPM block is appropriately estimated, the temperature of the electrode is considered to be correct enough. The deformation due to thermal expansion is negligible in case of the maximum temperature of 35 °C.

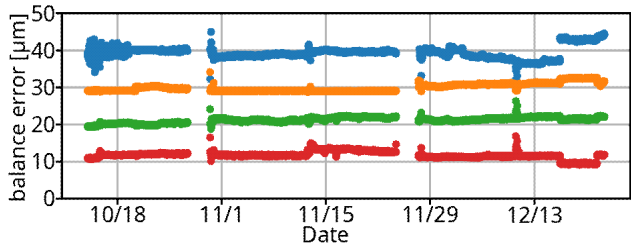

Figure 8: Trend graph of balance errors of 4 BPMs for 2.5 months.

SUMMARY

We have developed a high-resolution and highly stable BPM system for low-emittance upgrade of SPring-8. The BPM electrode and block was designed so that both enough signal intensity and enough electric center accuracy were obtained and that heat generation due to trapped modes was minimized. Some radiation-resistant coaxial cables were selected to prevent any drifts due to radiation damage of signal cables. For a readout electronics, we are developing original electronics based on the MicroTCA.4 standard and evaluating Libera Brilliance+. A beam test was performed by using a prototype BPM in the present SPring-8. The position resolution of 0.01 μm rms was obtained for the COD-mode and 70 μm rms for the SP-mode with a 100 pC single-bunch. The long-term stability was evaluated to be within 5 μm for a month. The temperature rise of the BPM block was also consistent with the results of the electromagnetic simulation and the thermal simulation. Thus, the developed BPM system satisfied the requirements for the SPring-8 upgrade.

REFERENCES

[1] SPring-8-II Conceptual Design Report, Nov. 2014, http://rsc.riken.jp/pdf/SPring-8-II.pdf

[2] CST Studio Suite, https://www.cst.com/

[3] M. Masaki *et al.*, "Design Optimization of Button-type BPM Electrode for the SPring-8 Upgrade", in *Proc. IBIC'16*, Barcelona, Spain, Sep. 2016, pp. 360–363, doi:10.18429/JACoW-IBIC2016-TUPG18

[4] ANSYS, https://www.ansys.com/

[5] T. Fujita *et al.*, "Long-term Stability of the Beam Position Monitors at SPring-8", In *Proc. IBIC'15*, Melbourne, Australia, Sep. 2015, pp. 359–363, doi:10.18429/JACoW-IBIC2015-TUPB020

[6] PICMG MicroTCA open standard, https://www.picmg.org/openstandards/microtca/

[7] Instrumentation Technologies, https://www.i-tech.si/

[8] T. Ohshima *et al.*, "Development of a New LLRF System Based on MicroTCA.4 for the SPring-8 Storage Ring", in *Proc. IPAC'17*, Copenhagen, Denmark, May 2017, pp. 3996–3999, doi:10.18429/JACoW-IPAC2017-THPAB117

Content from this work may be used under the terms of the CC BY 3.0 licence (© 2018). Any distribution of this work must maintain attribution to the author(s), title of the work, publisher, and DOI.